Letter

Plasmonic quantum nonlinear Hall effect in noncentrosymmetric two-dimensional materials

Riki Toshio * and Norio Kawakami
Department of Physics, Kyoto University, Kyoto 606-8502, Japan

(Received 25 August 2022; revised 22 October 2022; accepted 25 October 2022; published 4 November 2022)

We investigate an interplay between quantum geometrical effects and surface plasmons through surface plasmonic structures, based on an electron hydrodynamic theory. First we demonstrate that the quantum nonlinear Hall effect can be dramatically enhanced over a very broad range of frequency by utilizing plasmonic resonances and near-field effects of grating gates. Under the resonant condition, the enhancement becomes several orders of magnitude larger than the case without the nanostructures, while the peaks of high-harmonic plasmons expand broadly and emerge under the off-resonant condition, leading to a remarkably broad spectrum. Furthermore, we clarify a universal relation between the photocurrent induced by the Berry curvature dipole and the optical absorption, which is essential for computational material design of long-wavelength photodetectors. Next we discuss a novel mechanism of geometrical photocurrent, which originates from an anomalous force induced by oscillating magnetic fields and is described by the dipole moment of orbital magnetic moments of Bloch electrons in the momentum space. Our theory is relevant to two-dimensional quantum materials such as layered WTe_2 and twisted bilayer graphene, thereby providing a promising route toward a novel type of highly sensitive, broadband terahertz photodetector.

DOI: 10.1103/PhysRevB.106.L201301

Introduction. Quantum geometry [1–3] plays a crucial role in the linear/nonlinear optical responses of bulk crystals, as exemplified by natural optical activity [4–11], the bulk photovoltaic effect [12–16], and geometric photon drag [17]. These phenomena provide us with not only a deep insight into the band structure of crystals, but also a variety of functional optical devices, such as solar cells [18,19] and infrared/terahertz photodetectors [20–22]. For example, recently the quantum nonlinear Hall (QNLH) effect [23]—an intrinsic low-frequency photocurrent driven by the Berry curvature dipole—has been attracting much interest as a promising candidate for a broadband long-wavelength photodetector at room temperature [22,24].

Plasmonic nanostructures also provide us with another type of efficient and electrically tunable optical device [25–29]. Such a plasmonic nanodevice achieves its remarkable performance by utilizing the nonlocality and the plasmonic enhancement triggered by the nanostructures. In particular, surface plasmons inherent in two-dimensional (2D) layered systems, such as graphene, are known to have remarkably long lifetimes and electrically tunable dispersions in the terahertz or midinfrared region [30–32]. These properties are ideal for plasmonic devices, and thus a lot of papers have been devoted to investigating such applications as tunable terahertz photodetectors [33–36] and broadband absorbers [37–39].

Electron hydrodynamics, which is quickly growing into a mature field of condensed-matter physics [40–44], gives us a powerful tool to describe electronic collective modes [45–53] and nonlocality of optical responses [35,36,54–68]. Remarkable examples related with optical applications include the theory of the plasmonic instability [69–79] and the ratchet effect [80–88], both of which harness the plasma modes to realize highly efficient photovoltaic conversions. Interestingly, for the latter, the hydrodynamic signature has been observed very recently in bilayer graphene with an asymmetric dual-grating gate potential [87,88]. As a more recent development, the symmetry of crystals and quantum geometry give a new twist to the concept of electron hydrodynamics [51,68,89–108]. Indeed, in the past few years, a number of papers have addressed rich and novel hydrodynamic phenomena, represented by anisotropic viscosity effects [89–93]. Especially for noncentrosymmetric systems, it has been revealed that the quantum geometry causes anomalous driving forces over electron fluids, leading to unique hydrodynamic phenomena such as asymmetric Poiseuille flows [96] and nonreciprocal surface plasmons [102]. These frameworks enable us to investigate the interplay between quantum geometry and surface plasmons in novel materials, such as topological or van der Waals (vdW) materials [31,109–111]. These issues have not been addressed so far, except for several limited problems [45–48,102,112–116].

In this Letter, based on an electron hydrodynamics, we develop a generic theory of geometrical photocurrent in noncentrosymmetric 2D layered systems with periodic grating gates. First we demonstrate that the QNLH effect is enhanced dramatically by plasmonic resonances and near-field effects of grating gates, which is dubbed the *plasmonic QNLH effect*. It features multiple sharp peaks near the plasma frequencies, and it could be enhanced by several orders of magnitude over a very broad range of frequency. Furthermore, assuming more generic situations, we uncover a universal relation between the photocurrent induced by the Berry curvature dipole and

*toshio.riki.63c@st.kyoto-u.ac.jp

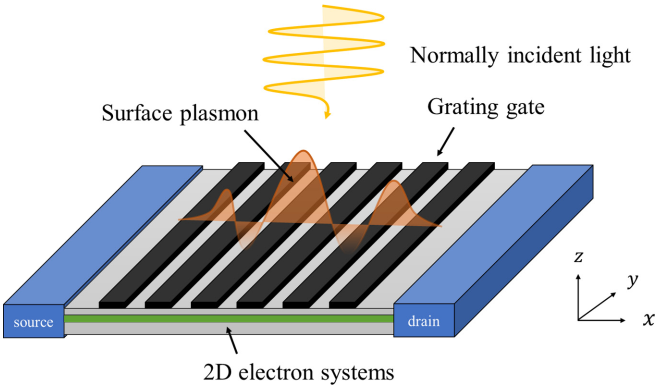

FIG. 1. Our setup for plasmonically driven geometrical photocurrent in noncentrosymmetric layered systems with periodic grating gate. Other types of experimental setups, such as plasmonic cavity or antenna, would be relevant to this work.

the optical absorption, which is essential for computational material design of long-wavelength photodetectors. Finally, we discuss another type of novel geometrical photocurrent, namely the *magnetically driven plasmonic photogalvanic effect*. This is a spatially dispersive contribution to the total photocurrent, and it originates from the anomalous driving force on electron fluids, which is described by the dipole moment of orbital magnetic moments in momentum space.

Setups. Let us specify our model to describe noncentrosymmetric layered systems with plasmonic grating gates (see Fig. 1). We assume that the grating gate spatially modulates the normally incident light $\boldsymbol{E}_0(t) = \mathrm{Re}[\tilde{\boldsymbol{E}}_0 e^{i\omega t}]$, leading to the spatially dispersive electric field in 2D electron systems [84,87]:

$$\boldsymbol{E}_{\rm in}(t,x) = [1 + \hat{h}\cos(qx+\phi)]\boldsymbol{E}_0(t), \tag{1}$$

where the diagonal matrix $\hat{h} = \mathrm{diag}\{h_x, h_y\}$ is a phenomenological parameter to determine the direction of the modulated electric field [117]. Especially when h_y is finite, Faraday's law results in the presence of an out-of-plane magnetic field,

$$B(t,x) = \frac{qh_y}{\omega}\sin(qx+\phi)\mathrm{Re}[-i\tilde{E}_{0y}e^{i\omega t}]. \tag{2}$$

Since the grating gate strongly confines the incident light into the $x-y$ plane with a fixed small wavelength, this magnetic field has non-negligible contributions especially in the low-frequency limit, leading to a novel mechanism of the photovoltaic effect as discussed below.

When the gate electrode is separated from the channel by an insulator thin film with thickness d and gate-to-channel capacity $C = \varepsilon/4\pi d$, the 2D electron concentration $n(\boldsymbol{r},t)$ is approximately determined by the local gate-to-channel voltage $U(\boldsymbol{r},t)$: $n(\boldsymbol{r},t) = \frac{C}{e}U(\boldsymbol{r},t)$. Such an approximation is often referred to as a gradual channel approximation [69,118], which is valid for smooth perturbation with $qd \ll 1$. In summary, the total electric field is given by the sum of the incident light $\boldsymbol{E}_{\rm in}$ and the field coming from the density perturbation: $\boldsymbol{E} = \boldsymbol{E}_{\rm in} + (e/C)\nabla n$.

Next, let us consider the dynamics of electron fluids in noncentrosymmetric crystals with time-reversal symmetry. In this paper, we focus on the hydrodynamic regime, where the rate of electron-electron scatterings $1/\tau_e$ exceeds that of other momentum-relaxing scatterings $1/\tau$, and thereby the total electron momentum can be regarded as a long-lived quantity [40–43,119]. Under these conditions, the electron dynamics is described by an emergent hydrodynamic theory, whose form crucially depends on the symmetry of the systems [51,68,89–96,98,100–107]. As also mentioned later, such a hydrodynamic behavior of electrons has been observed in transport experiments in various materials, and it has attracted a lot of interest in the past few years [43,44].

For noncentrosymmetric electron fluids with parabolic dispersion near some valley α, the formulation of electron hydrodynamics is obtained in Refs. [96,102]. Under some reasonable approximations [120], we can transform the hydrodynamic equations for our analysis as follows:

$$\begin{aligned}&\frac{\partial \boldsymbol{u}}{\partial t} + (\boldsymbol{u}\cdot\nabla)\boldsymbol{u} + \frac{\nabla P}{mn} + \frac{e}{m}(\boldsymbol{E} + \boldsymbol{u}\times\boldsymbol{B})\\ &\quad + \frac{\boldsymbol{M}}{n}\left(\frac{\partial B}{\partial t}\right) = -\frac{\boldsymbol{u}}{\tau},\\ &\frac{\partial n}{\partial t} + \div(n\boldsymbol{u}) = 0,\end{aligned} \tag{3}$$

where n and ρ are the density of particles and mass, B is an applied static magnetic field, $\boldsymbol{u}$ is the velocity field of the electron fluid, and P is the pressure. The last term on the left-hand side in the first equation is first derived in Ref. [102], and it represents a geometrical anomalous force due to oscillating magnetic fields, which is closely related with the so-called gyrotropic magnetic effect [7,9–11]. Here $\boldsymbol{M}$ is a geometrical pseudovector, and it is defined as the dipole component of orbital magnetic moments of Bloch electrons in momentum space:

$$\boldsymbol{M} = \sum_\alpha \boldsymbol{M}^\alpha, \quad M_i^\alpha \equiv \int [d\boldsymbol{p}]\frac{\partial m_z^\alpha}{\partial p_i} f_{0\alpha},$$

where $f_{0\alpha} = [1 + e^{-\beta[\varepsilon_\alpha(\boldsymbol{p})-\mu]}]^{-1}$ is the Fermi distribution function at the valley α, $m_z^\alpha(\boldsymbol{p})$ is the orbital magnetic moment of Bloch wave packets [1], and we have introduced the notation $\int[d\boldsymbol{p}] \equiv \int d\boldsymbol{p}/(2\pi\hbar)^d$ [121].

Here it is notable that the velocity field itself is not an observable quantity. We have to relate the velocity field $\boldsymbol{u}$ with the observable electric current as follows [96,102]:

$$\boldsymbol{j} = -en\boldsymbol{u} - \frac{me^2}{\hbar}(\boldsymbol{D}\cdot\boldsymbol{u} + YB)\cdot(\boldsymbol{E}\times\hat{\mathbf{e}}_z) + \cdots, \tag{4}$$

where $\boldsymbol{D}$ is another geometric pseudovector, which is often referred to as the Berry curvature dipole (BCD) [23], defined as

$$\boldsymbol{D} = \sum_\alpha \boldsymbol{D}^\alpha, \quad D_i^\alpha \equiv \int [d\boldsymbol{p}]\frac{\partial \Omega_{\alpha,z}}{\partial p_i} f_{0\alpha},$$

and Y is a geometrical scalar coefficient,

$$Y = \sum_\alpha Y^\alpha, \quad Y^\alpha = -\frac{1}{m}\int [d\boldsymbol{p}]\Omega_z^\alpha m_z^\alpha \partial_\epsilon f_0(\epsilon_0).$$

Here $\Omega_z^\alpha(\boldsymbol{p})$ is the Berry curvature of Bloch electrons in the valley α, and it is defined as $\Omega_z^\alpha = \partial_x A_y^\alpha - \partial_y A_x^\alpha$ with the Berry connection $\boldsymbol{A}^\alpha = i\langle u_{\alpha\boldsymbol{p}}|\nabla_{\boldsymbol{p}} u_{\alpha\boldsymbol{p}}\rangle$ and the Bloch wave function $u_{\alpha\boldsymbol{p}}$ [1]. We note that "$\cdots$" in Eq. (5) denotes the rotational currents, which causes several remarkable phenomena such as vorticity-induced anomalous current [96], but it does not contribute to the analysis in this work. Importantly, from symmetry considerations, we find that electron systems with time-reversal symmetry have to be noncentrosymmetric to obtain finite values of m_z^α and Ω_z^α [1]. Moreover, since crystal symmetries impose further strong restrictions on the geometrical pseudovectors $\boldsymbol{M}$ and $\boldsymbol{D}$, we have to break any rotational symmetry about the z-axis and reduce the number of in-plane mirror lines to be less than two for these vectors to be finite [23,96].

Plasmonic QNLH effect. Here we demonstrate that the spatial modulation by grating gates gives rise to the plasmonic enhancement of the QNLH effect. Interestingly, Ref. [22] suggested recently that the QNLH effect has great potential for a broadband long-wavelength photodetector with small noise-equivalent power and remarkably high internal responsivity, which is defined as the gain per absorbed power, in a broad range of frequency. However, since its spectrum has a Lorentzian shape located at $\omega = 0$ with the half-width $1/\tau$, its external responsivity, i.e., its gain per incident power, rapidly decreases as ω^{-2} at frequencies $\omega \gg 1/\tau$, while the internal responsivity maintains a good value independent of the frequencies. Therefore, it is still an open problem how to improve the external responsivity of the QNLH effect at moderately high frequencies and whether its internal responsivity remains intact even in plasmonic resonances or not. In what follows, we reveal that plasmonic resonance dramatically improves the external responsivity (or the nonlinear susceptibility) by several orders of magnitude in a broad regime of frequency over $1/\tau$.

By performing a simple second-order perturbative analysis, we can easily solve the hydrodynamic equations (3) and obtain the total photocurrent, which can be decomposed into two components coming from different novel mechanisms as follows (for the detailed derivation and expression, see the Supplemental Material [120]):

$$\boldsymbol{j}_{\mathrm{DC}} = \boldsymbol{j}_{\mathrm{DC}}^{\mathrm{BCD}} + \boldsymbol{j}_{\mathrm{DC}}^{\mathrm{MPP}}, \tag{5}$$

where $\boldsymbol{j}_{\mathrm{DC}}^{\mathrm{BCD}}$ is a photocurrent originating from the BCD vector $\boldsymbol{D}$, which is understood as a plasmonic version of the so-called QNLH effect [23]. On the other hand, $\boldsymbol{j}_{\mathrm{DC}}^{\mathrm{MPP}}$ is another novel type of geometrical photocurrent, which comes from several nonlinear terms in Eq. (3), such as the inertia term $(\boldsymbol{u}\cdot\nabla)\boldsymbol{u}$. As discussed later in more detail, since $\boldsymbol{j}_{\mathrm{DC}}^{\mathrm{MPP}}$ is induced by an external oscillating magnetic field in Eq. (2), we will hereafter refer to this contribution as the *magnetically driven plasmonic photogalvanic (MPP) effect*.

Here let us consider x-polarized incident light $\tilde{\boldsymbol{E}}_0 = (\tilde{E}_{0x}, 0, 0)$. In this case, the total photocurrent is exactly attributed only to the contribution of the QNLH term $\boldsymbol{j}_{\mathrm{DC}}^{\mathrm{BCD}}$ and described by a simple beautiful form

$$\boldsymbol{j}_{\mathrm{DC}} = \boldsymbol{j}_{\mathrm{DC}}^{\mathrm{BCD}} = -\frac{e^3}{2\hbar}\frac{\tau\beta_\omega}{1+(\omega\tau)^2}D_x|\tilde{E}_{0x}|^2\hat{\boldsymbol{e}}_y, \tag{6}$$

where $\hat{\boldsymbol{e}}_y$ is a unit vector in the y-direction, β_ω is an amplification factor due to the plasmonic resonance,

$$\beta_\omega = 1 + \frac{\tilde{\omega}^2(1+\tilde{\tau}^2\tilde{\omega}^2)h_x^2}{2[\tilde{\tau}^2(\tilde{\omega}^2-1)^2+\tilde{\omega}^2]}, \tag{7}$$

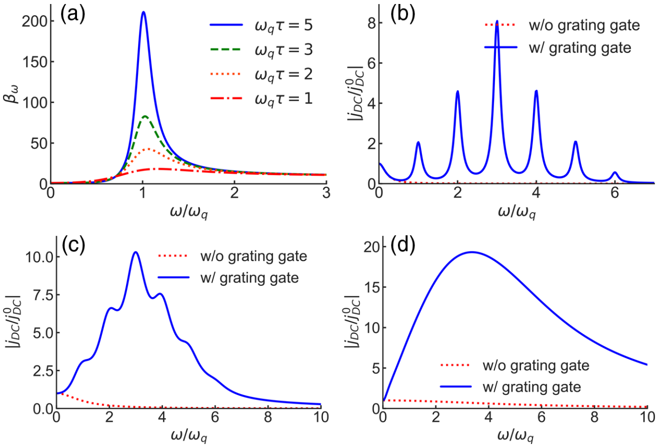

FIG. 2. Frequency dependence of the enhancement factor β_ω and the plasmonic QNLH current $j_{\mathrm{DC}} = j_{\mathrm{DC}}^{\mathrm{BCD}}$. (a) We plot the enhancement factor, Eq. (10), which comes from only one plasmonic peak, with $h_x = 4$ and various values of $\tilde{\tau} = \omega_q\tau$. (b)–(d) Considering the enhancement factor, Eq. (8), due to high-harmonic plasmons, we plot the plasmonic QNLH current, Eq. (6), normalized by $j_{\mathrm{DC}}^0 \equiv j_{\mathrm{DC}}(\omega=0)$. We set the parameter $\tilde{\tau} = \omega_q\tau$ as (b) $\omega_q\tau = 5$, (c)$\omega_q\tau = 1$, and (d) $\omega_q\tau = 0.2$ and, for demonstration purposes, we assume phenomenologically that $(h_x^{(1)}, h_x^{(2)}, h_x^{(3)}, h_x^{(4)}, h_x^{(5)}, h_x^{(6)}) = (2, 3, 4, 3, 2, 1)$ and $h^{(i)} = 0$ $(i \geqslant 7)$. For comparison, we also plot the spectrum of the usual QNLH current with a red dotted line.

and we have introduced two dimensionless parameters: $\tilde{\tau} = \omega_q\tau$ and $\tilde{\omega} = \omega/\omega_q$. Here ω_q is the plasmon frequency $\omega_q = sq$, and s is the group velocity of the plasmon. This is one of our main results in this work, and we refer to it as the *plasmonic QNLH effect*. In Fig. 2(a), we have plotted the spectrum of β_ω for various values of $\tilde{\tau}$.

In the low-frequency limit ($\tilde{\omega} \to 0$), the amplification factor β_ω approaches 1 and Eq. (6) becomes equivalent to that in Ref. [23], which means that the original peak of the QNLH effect at $\omega = 0$ remains intact regardless of the existence of the grating gate. On the other hand, at the plasmon frequency $\omega = \omega_q$, it features another sharp peak with a width $\Delta\omega \sim 1/\tau$ in the resonant regime ($\tilde{\tau} \gg 1$), and the amplitude of the QNLH current is strongly enhanced by the dimensionless factor $|\beta_{\omega_q}| \sim |h_x\tilde{\tau}|^2/2$, compared to the case without the grating gate. In particular, by utilizing near-field enhancement of gold grating gates, it is possible for the grating factor h_x to be comparable to or much larger than 1 ($h_x \gg 1$) [85,122,123]. This means that the QNLH current could be enhanced by several orders of magnitude under the resonant condition ($\tilde{\tau} \gg 1$).

In the discussion so far, we have focused on a specific harmonic mode with the wave number q in Eq. (1) for simplicity. However, we note that, in general, the grating gate creates high-harmonic modulations of in-plane electric fields with the wave numbers mq $(m = 2, 3, \dots)$ [81,124–126], which can be described as

$$E_{\mathrm{in},i}(t,x) = \left[1 + \sum_{m=1}^{\infty}\hat{h}_i^{(m)}\cos(mqx+\phi_i^{(m)})\right]E_{0i}(t).$$

These modulations result in multiple plasmonic resonant peaks at $\omega = \omega_{nq}$ $(n = \pm1, \pm2, \dots)$, leading to a remarkably broadband photocurrent spectrum. In particular, since the result in Eq. (6) does not depend on the phases $\phi_i^{(m)}$ and the signs of $h_x^{(m)}$, each contribution to the photocurrent from high-harmonic plasmons flows in the same direction, and thus the total photocurrent is strongly enhanced. This is in sharp contrast to the case of the so-called ratchet effect [81,84], which is strongly dependent on these parameters, and thus photocurrent contribution from each plasma mode often cancels those from the other modes. In conclusion, enhancement factor (10) is modified by high-harmonic plasmons as follows:

$$\beta_\omega = 1 + \sum_{m=1}^{\infty} \frac{\tilde{\omega}^2(1+\tilde{\tau}^2\tilde{\omega}^2)\big(h_x^{(m)}\big)^2}{2[m^2\tilde{\tau}^2(\tilde{\omega}^2-m^2)^2+\tilde{\omega}^2]}. \tag{8}$$

In Figs. 2(b)–2(d) we have plotted the spectrum of the plasmonic QNLH current (blue line), and we compared it with that of the normal QNLH effect. From these figures, we find that the QNLH current is dramatically enhanced by several orders of amplitude, over a very broad range of frequency above the original frequency threshold $1/\tau$. Similar enhancement effects due to high-harmonic plasma modes have previously been discussed in the context of terahertz light absorption [124,127,128] and the plasmonic ratchet effect [85,122].

Universal internal responsivity. Here, assuming more general situations, we elucidate a universal relation between the photocurrent induced by the BCD and the light absorption by 2D electron systems. First, in general, the BCD-induced photocurrent is obtained from Eq. (5) in the following form:

$$\boldsymbol{j}_{\mathrm{DC}}^{\mathrm{BCD}} = -\frac{me^2}{\hbar}\langle[\boldsymbol{D}\cdot\boldsymbol{u}(\boldsymbol{r},t)][\boldsymbol{E}(\boldsymbol{r},t)\times\hat{\boldsymbol{e}}_z]\rangle_{t,\boldsymbol{r}},$$

where $\langle\cdots\rangle_{t,\boldsymbol{r}}$ denotes the time and space averaging over the periods. Especially for x-polarized incident light, it leads to $\boldsymbol{j}_{\mathrm{DC}}^{\mathrm{BCD}} = \frac{me^2}{\hbar}D_x\langle u_xE_x\rangle_{t,\boldsymbol{r}}\hat{\boldsymbol{e}}_y$. On the other hand, the optical power absorbed by 2D electron systems can be calculated as $\mathcal{P} = S\langle j_xE_x\rangle_{t,\boldsymbol{r}}$, where $S = L_xL_y$ is the area of our system and L_i is the sample's size in the i-direction. In the linear order of external perturbations, the electric current is related with the velocity field as $j_x = -en_0u_x$ from Eq. (5), where n_0 is the equilibrium particle density. Combining these formulas, we reach the desired universal relation between $\boldsymbol{j}_{\mathrm{DC}}^{\mathrm{BCD}}$ and $\mathcal{P}$ as follows:

$$\boldsymbol{j}_{\mathrm{DC}}^{\mathrm{BCD}} = -\frac{emD_x\mathcal{P}}{\hbar n_0 S}\hat{\boldsymbol{e}}_y. \tag{9}$$

This relation means that the plasmonic QNLH effect discussed above comes from the plasmonic enhancement of the total optical absorption by the grating gate. As can be understood from the derivation, Eq. (9) will be satisfied in more generic situations beyond our 2D grating model, such as plasmonic cavities [129–132] or antennas [34,133], as long as the frequency is low enough for interband transitions to be negligible [134]. Here we note that, as is easily checked from the formula, Eq. (9) does not hold for the circular photogalvanic current induced by the BCD [120]. This means that higher efficiency can be achieved for circularly polarized light, which is analogous to recent proposals in Refs. [135,136].

From Eq. (9), we can immediately obtain the internal current responsivity of the BCD-induced Hall photocurrent, which is one of the most important figures of merit quantifying the performance of THz detectors [33], and it is defined as the current gain per absorbed light power,

$$\mathcal{R}_I \equiv \frac{|I_y|}{\mathcal{P}} = \left|\frac{emD_x}{\hbar n_0 L_y}\right| \quad \big(I_y = j_{\mathrm{DC},y}^{\mathrm{BCD}}L_x\big). \tag{10}$$

This is another important result in this paper. Equation (10) states that the responsivity is entirely determined by the band structure (and the carrier density) of electron systems, and completely independent of incident frequencies and their environment, such as grating or cavity structures. Clearly, this property is very beneficial for the computational material design of terahertz-infrared photodetectors. To realize a high-performance photodetector utilizing the BCD-induced photocurrent, first we should search quantum materials with a colossal effective mass m and BCD by performing *ab initio* calculations or experiments, and then we should improve their optical absorption by designing those promising materials with some plasmonic or cavity structures.

For the latter purpose, 2D layered materials, which are very adaptable to various device designs, seem to be more advantageous than 3D bulk materials. Recent experiments [137] have reported that the voltage responsivity of bilayer WTe_2 reaches a value of 2×10^4 V/W^{-1} around $\omega\sim100$ Hz at $T = 10$ K, which is notably large and comparable to the best values in existing rectifiers [137,138]. Furthermore, Ref. [139] has theoretically suggested that strained twisted bilayer graphene achieves a further large responsivity that is 20 times larger than the above values. However, since these materials work well only at low temperature, further investigations of promising materials, which show a remarkably large value of the BCD, will be needed to realize terahertz photodetectors working at room temperature.

Magnetically driven plasmonic photogalvanic effect. Next let us consider a novel type of photocurrent, $\boldsymbol{j}_{\mathrm{DC}}^{\mathrm{MPP}}$, obtained in Eq. (8), which is regarded as a spatially dispersive correction to the total photocurrent and is proportional to q^2 or q^4. For this reason, this effect is peculiar to spatially structured systems like our grating model, and it does not appear in spatially uniform cases.

As shown in detail in the Supplemental Material [120], the MPP effect originates from an anomalous driving force induced by oscillating magnetic fields [$\propto \boldsymbol{M}(\partial B/\partial t)$] in Eq. (3), and thus it is described by the geometrical pseudovector, $\boldsymbol{M}$, i.e., the dipole moment of orbital magnetic moments of Bloch electrons in momentum space (for the detailed derivation and expression, see the Supplemental Material [120]). In particular, at plasmon frequencies, the MPP current also has a sharp peak, as in the case of the plasmonic QNLH effect, and the peak amplitude is obtained under the resonant condition ($\tilde{\tau}\gg1$) as follows [140]:

$$\boldsymbol{j}_{\mathrm{DC}}^{\mathrm{MPP}}(\omega=\omega_q) = \frac{e^2\tau}{4ms^2}[\tilde{\tau}h_xh_y\mathcal{F}_z(\boldsymbol{M}+2M_x\hat{\boldsymbol{e}}_x) + \tilde{\tau}^2h_xh_y\mathcal{L}_{xy}M_x\hat{\boldsymbol{e}}_x] + O(\tilde{\tau}^0).$$

Here we have introduced $\mathcal{F}_z = \frac{i}{2}(\tilde{E}_{0x}\tilde{E}_{0y}^* - \tilde{E}_{0y}\tilde{E}_{0x}^*)$ and $\mathcal{L}_{xy} = \frac{1}{2}(\tilde{E}_{0x}\tilde{E}_{0y}^* + \tilde{E}_{0y}\tilde{E}_{0x}^*)$, each of which represents a circular photogalvanic effect and a linear photogalvanic effect. Focusing on its circular photogalvanic effect in the x-direction, the value of MPP current is around 0.01 nA/W with typical values of parameters $m\sim m_e$, $s\sim1\times10^6$ m/s, $\tau\sim1\times10^{-12's}$, and an estimated value of M_x obtained in Ref. [102] for strained graphene, $M_x \sim 3 \times 10^{17}$ s A/kg m, assuming the resonant case $|\tilde{\tau} h_x h_y| \gtrsim 10$. Although this is much smaller than the measured value of QNLH current (∼100 nA/W) in monolayer WTe_2 [141] around $\omega \simeq 30$ THz at 150 K, we might be able to improve the MPP current further by seeking materials with a much larger value of $\boldsymbol{M}$. In such a situation, since the plasmonic term of the BCD-induced circular photocurrent is proportional to $\omega^2 - \omega_q^2$ and thus vanishes at the plasmon frequency, the MPP effect will dominate the total photocurrent. This might be a good optical probe for the geometrical structures of Bloch electrons in 2D quantum systems.

Discussion. Here we briefly discuss possible candidates to observe the novel types of plasmonic photocurrents obtained in this work. In the past few years, many pieces of evidence for hydrodynamic electron flow have been reported in various materials, including monolayer/bilayer graphene [142–147], GaAs quantum wells [148–153], 2D monovalent layered metal $PdCoO_2$ [154], Weyl semimetal WP_2 [155], and WTe_2 [156–158]. Among these materials, promising candidates for our work are graphene with some deformation and layered transition-metal dichalcogenide WTe_2. These materials have crystal symmetries low enough to exhibit intriguing optical phenomena, such as the QNLH effect [23], which is required for the geometrical pseudovectors $\boldsymbol{D}$ and $\boldsymbol{M}$ to be finite. As a matter of fact, the QNLH effect itself has already been observed in layered WTe_2 [137,141,159,160] and artificially corrugated bilayer graphene [161]. In particular, bilayer WTe_2 is reported to show remarkably high responsivity [137], as was already mentioned, and further dramatic enhancement of the BCD is suggested by twisting the two layers in Ref. [162].

Another possible candidate is the (110) quantum well in GaAs, since it also has crystal symmetries low enough to exhibit the QNLH effect [163–166], and another type of GaAs quantum well has already exhibited various hydrodynamic signatures [148–153]. Furthermore, twisted bilayer graphene, a novel layered system that has been attracting great interest recently, might also be a candidate for our work, since this material is theoretically suggested to realize the hydrodynamic regime [167] and to show a remarkably high responsivity of the QNLH effect [139].

Finally, we give a brief discussion about the viscosity effect on our results [120]. In the context of electron hydrodynamics, viscosity is regarded as a key ingredient to characterize electron dynamics in the hydrodynamic regime. Actually, many recent experiments have been devoted to measurements of the signature of viscosity in nonlocal transport phenomena [142,147,151–155]. By turning on the viscosity term phenomenologically in Eq. (3), we find that the width of plasmonic peaks in Eq. (9) is modified from $1/\tau$ to $1/\tau + (\nu + \zeta)q^2$, where ν and ζ are the kinetic viscosity and the bulk viscosity. This means that, for typical values of parameters $\tau = 1 \times 10^{-12}$ s^{-1} and $\nu = 1 \times 10^{-1}$ $m^2 s^{-1}$ [142], viscosity causes non-negligible contributions to the plasmon lifetime when the cycle length $L = 2\pi/q$ becomes μm-order or less. Consequently, it might be possible to optically probe mysterious aspects of strongly correlated electron systems such as twisted bilayer graphene [168–171], through the peculiar temperature dependence of the plasmon lifetime, since the electron viscosity behaves as $\nu \sim v_F l_{ee} \propto 1/T^2$ in Fermi liquids [155,172,173], while $\nu \propto 1/T$ in typical non-Fermi-liquids [42,155,174,175].

Conclusion. In summary, based on an electron hydrodynamic theory, we have formulated plasmonically driven geometrical photocurrents in noncentrosymmetric 2D layered systems with periodic grating gates. Our framework can be generalized to various types of problems in plasmonics, such as plasmonic responses of 1D vdW materials [176,177], gate-controlled optical activity [178], and plasmon-to-current converters [83,179]. This provide us with a way to investigate the role of quantum geometry in plasmonics, leading to a promising route toward a novel type of highly sensitive, broadband, and electrically controllable terahertz plasmonic device.

Acknowledgments. We would like to express our special thanks to H. Watanabe and K. Tanaka for useful comments. We are also grateful to G. Tatara, H. Funaki, R. Sano, and A. Daido for valuable discussions. This work is partly supported by JSPS KAKENHI (Grants No. JP20J22612 and No. JP19H01838).

[1] D. Xiao, M.-C. Chang, and Q. Niu, Rev. Mod. Phys. **82**, 1959 (2010).
[2] Q. Ma, A. G. Grushin, and K. S. Burch, Nat. Mater. **20**, 1601 (2021).
[3] In this paper, we use the words "quantum geometry" and "quantum geometrical" to refer to nontrivial (geometrical) structures of Bloch wave functions in $\boldsymbol{p}$-space and the related phenomena, which are described by some geometrical quantities such as the so-called Berry curvature [2]. For the mathematical details from a geometrical perspective, for example, see Refs. [1,15,180].
[4] A. Malashevich and I. Souza, Phys. Rev. B **82**, 245118 (2010).
[5] J. Orenstein and J. E. Moore, Phys. Rev. B **87**, 165110 (2013).
[6] S. Zhong, J. Orenstein, and J. E. Moore, Phys. Rev. Lett. **115**, 117403 (2015).
[7] J. Ma and D. A. Pesin, Phys. Rev. B **92**, 235205 (2015).
[8] P. Hosur and X.-L. Qi, Phys. Rev. B **91**, 081106(R) (2015).
[9] S. Zhong, J. E. Moore, and I. Souza, Phys. Rev. Lett. **116**, 077201 (2016).
[10] F. Flicker, F. de Juan, B. Bradlyn, T. Morimoto, M. G. Vergniory, and A. G. Grushin, Phys. Rev. B **98**, 155145 (2018).
[11] Y.-Q. Wang, T. Morimoto, and J. E. Moore, Phys. Rev. B **101**, 174419 (2020).
[12] C. Aversa and J. E. Sipe, Phys. Rev. B **52**, 14636 (1995).
[13] J. E. Sipe and A. I. Shkrebtii, Phys. Rev. B **61**, 5337 (2000).
[14] N. Nagaosa and T. Morimoto, Adv. Mater **29**, 1603345 (2017).
[15] J. Ahn, G.-Y. Guo, and N. Nagaosa, Phys. Rev. X **10**, 041041 (2020).
[16] H. Watanabe and Y. Yanase, Phys. Rev. X **11**, 011001 (2021).
[17] L.-k. Shi, D. Zhang, K. Chang, and J. C. W. Song, Phys. Rev. Lett. **126**, 197402 (2021).
[18] L. Z. Tan, F. Zheng, S. M. Young, F. Wang, S. Liu, and A. M. Rappe, npj Comput. Mater. **2**, 16026 (2016).

[19] A. M. Cook, B. M. Fregoso, F. de Juan, S. Coh, and J. E. Moore, Nat. Commun. **8**, 14176 (2017).
[20] J. Liu, F. Xia, D. Xiao, F. J. García de Abajo, and D. Sun, Nat. Mater. **19**, 830 (2020).
[21] H. Isobe, S.-Y. Xu, and L. Fu, Sci. Adv. **6**, eaay2497 (2020).
[22] Y. Zhang and L. Fu, Proc. Natl. Acad. Sci. USA **118**, e2100736118 (2021).
[23] I. Sodemann and L. Fu, Phys. Rev. Lett. **115**, 216806 (2015).
[24] Z. Z. Du, H.-Z. Lu, and X. C. Xie, Nat. Rev. Phys. **3**, 744 (2021).
[25] H. A. Atwater and A. Polman, Nat. Mater. **9**, 205 (2010).
[26] K. Yao and Y. Liu, Nanotechnol. Rev. **3**, 177 (2014).
[27] T. Low and P. Avouris, ACS Nano **8**, 1086 (2014).
[28] M. Hentschel, M. Schferling, X. Duan, H. Giessen, and N. Liu, Sci. Adv. **3**, e1602735 (2017).
[29] W. Yang, Q. Liu, H. Wang, Y. Chen, R. Yang, S. Xia, Y. Luo, L. Deng, J. Qin, H. Duan, and L. Bi, Nat. Commun. **13**, 1719 (2022).
[30] L. Ju, B. Geng, J. Horng, C. Girit, M. Martin, Z. Hao, H. A. Bechtel, X. Liang, A. Zettl, Y. R. Shen, and F. Wang, Nat. Nanotechnol. **6**, 630 (2011).
[31] D. N. Basov, M. M. Fogler, and F. J. G. de Abajo, Science **354**, aag1992 (2016).
[32] Y. Li, Z. Li, C. Chi, H. Shan, L. Zheng, and Z. Fang, Adv. Sci. **4**, 1600430 (2017).
[33] F. H. L. Koppens, T. Mueller, P. Avouris, A. C. Ferrari, M. S. Vitiello, and M. Polini, Nat. Nanotechnol. **9**, 780 (2014).
[34] D. A. Bandurin, D. Svintsov, I. Gayduchenko, S. G. Xu, A. Principi, M. Moskotin, I. Tretyakov, D. Yagodkin, S. Zhukov, T. Taniguchi, K. Watanabe, I. V. Grigorieva, M. Polini, G. N. Goltsman, A. K. Geim, and G. Fedorov, Nat. Commun. **9**, 5392 (2018).
[35] V. Ryzhii, T. Otsuji, and M. Shur, Appl. Phys. Lett. **116**, 140501 (2020).
[36] Y. Zhang and M. S. Shur, J. Appl. Phys. **129**, 053102 (2021).
[37] S. Ke, B. Wang, and P. Lu, in *2015 IEEE MTT-S International Microwave Workshop Series on Advanced Materials and Processes for RF and THz Applications (IMWS-AMP)* (IEEE, Piscataway, NJ, 2015), pp. 1–1.
[38] K. Chaudhuri, M. Alhabeb, Z. Wang, V. M. Shalaev, Y. Gogotsi, and A. Boltasseva, ACS Photon. **5**, 1115 (2018).
[39] J. Huang, J. Li, Y. Yang, J. Li, J. Li, Y. Zhang, and J. Yao, Opt. Express **28**, 17832 (2020).
[40] B. N. Narozhny, I. V. Gornyi, A. D. Mirlin, and J. Schmalian, Ann. Phys. **529**, 1700043 (2017).
[41] A. Lucas and K. C. Fong, J. Phys.: Condens. Matter **30**, 053001 (2018).
[42] B. N. Narozhny, Ann. Phys. **411**, 167979 (2019).
[43] M. Polini and A. K. Geim, Phys. Today **73**(6), 28 (2020).
[44] B. N. Narozhny, La Rivista del Nuovo Cimento **45**, 661 (2022).
[45] A. Principi, M. I. Katsnelson, and G. Vignale, Phys. Rev. Lett. **117**, 196803 (2016).
[46] E. V. Gorbar, V. A. Miransky, I. A. Shovkovy, and P. O. Sukhachov, Phys. Rev. Lett. **118**, 127601 (2017).
[47] Y. Zhang, B. Guo, F. Zhai, and W. Jiang, Phys. Rev. B **97**, 115455 (2018).
[48] S. S.-L. Zhang and G. Vignale, Phys. Rev. B **97**, 224408 (2018).
[49] D. Svintsov, Phys. Rev. B **97**, 121405(R) (2018).
[50] P. O. Sukhachov, E. V. Gorbar, I. A. Shovkovy, and V. A. Miransky, J. Phys.: Condens. Matter **30**, 275601 (2018).
[51] E. V. Gorbar, V. A. Miransky, I. A. Shovkovy, and P. O. Sukhachov, Phys. Rev. B **97**, 121105(R) (2018).
[52] B. N. Narozhny, I. V. Gornyi, and M. Titov, Phys. Rev. B **103**, 115402 (2021).
[53] K. Kapralov and D. Svintsov, Phys. Rev. B **106**, 115415 (2022).
[54] S. Raza, S. I. Bozhevolnyi, M. Wubs, and N. A. Mortensen, J. Phys.: Condens. Matter **27**, 183204 (2015).
[55] M. Mendoza, H. J. Herrmann, and S. Succi, Sci. Rep. **3**, 1052 (2013).
[56] D. Forcella, J. Zaanen, D. Valentinis, and D. van der Marel, Phys. Rev. B **90**, 035143 (2014).
[57] W. Yan, Phys. Rev. B **91**, 115416 (2015).
[58] Z. Sun, D. N. Basov, and M. M. Fogler, Phys. Rev. B **97**, 075432 (2018).
[59] Z. Sun, D. N. Basov, and M. M. Fogler, Proc. Natl. Acad. Sci. USA **115**, 3285 (2018).
[60] P. S. Alekseev, Phys. Rev. B **98**, 165440 (2018).
[61] P. S. Alekseev and A. P. Alekseeva, Phys. Rev. Lett. **123**, 236801 (2019).
[62] S. O. Potashin, V. Y. Kachorovskii, and M. S. Shur, Phys. Rev. B **102**, 085402 (2020).
[63] M. W. Shabbir and M. N. Leuenberger, Sci. Rep. **10**, 17540 (2020).
[64] P. S. Alekseev and A. P. Alekseeva, arXiv:2105.01035.
[65] L. F. Man, W. Xu, Y. M. Xiao, H. Wen, L. Ding, B. Van Duppen, and F. M. Peeters, Phys. Rev. B **104**, 125420 (2021).
[66] F. De Luca, M. Ortolani, and C. Ciracì, Phys. Rev. B **103**, 115305 (2021).
[67] Y. A. Pusep, M. D. Teodoro, V. Laurindo, E. R. Cardozo de Oliveira, G. M. Gusev, and A. K. Bakarov, Phys. Rev. Lett. **128**, 136801 (2022).
[68] D. Valentinis, G. Baker, D. A. Bonn, and J. Schmalian, arXiv:2204.13344.
[69] M. Dyakonov and M. Shur, Phys. Rev. Lett. **71**, 2465 (1993).
[70] M. Dyakonov and M. Shur, IEEE Trans. Electron Devices **43**, 380 (1996).
[71] S. A. Mikhailov, Phys. Rev. B **58**, 1517 (1998).
[72] L. Vicarelli, M. S. Vitiello, D. Coquillat, A. Lombardo, A. C. Ferrari, W. Knap, M. Polini, V. Pellegrini, and A. Tredicucci, Nat. Mater. **11**, 865 (2012).
[73] A. Tomadin and M. Polini, Phys. Rev. B **88**, 205426 (2013).
[74] D. Spirito, D. Coquillat, S. L. De Bonis, A. Lombardo, M. Bruna, A. C. Ferrari, V. Pellegrini, A. Tredicucci, W. Knap, and M. S. Vitiello, Appl. Phys. Lett. **104**, 061111 (2014).
[75] I. Torre, A. Tomadin, R. Krahne, V. Pellegrini, and M. Polini, Phys. Rev. B **91**, 081402(R) (2015).
[76] C. B. Mendl and A. Lucas, Appl. Phys. Lett. **112**, 124101 (2018).
[77] C. B. Mendl, M. Polini, and A. Lucas, Appl. Phys. Lett. **118**, 013105 (2021).
[78] P. Cosme and H. Teras, Appl. Phys. Lett. **118**, 131109 (2021).
[79] J. Crabb, X. Cantos-Roman, J. M. Jornet, and G. R. Aizin, Phys. Rev. B **104**, 155440 (2021).
[80] V. V. Popov, D. V. Fateev, T. Otsuji, Y. M. Meziani, D. Coquillat, and W. Knap, Appl. Phys. Lett. **99**, 243504 (2011).

[81] P. Olbrich, J. Karch, E. L. Ivchenko, J. Kamann, B. März, M. Fehrenbacher, D. Weiss, and S. D. Ganichev, Phys. Rev. B **83**, 165320 (2011).
[82] E. L. Ivchenko and S. D. Ganichev, JETP Lett. **93**, 673 (2011).
[83] V. V. Popov, Appl. Phys. Lett. **102**, 253504 (2013).
[84] I. V. Rozhansky, V. Y. Kachorovskii, and M. S. Shur, Phys. Rev. Lett. **114**, 246601 (2015).
[85] P. Olbrich, J. Kamann, M. König, J. Munzert, L. Tutsch, J. Eroms, D. Weiss, M.-H. Liu, L. E. Golub, E. L. Ivchenko, V. V. Popov, D. V. Fateev, K. V. Mashinsky, F. Fromm, T. Seyller, and S. D. Ganichev, Phys. Rev. B **93**, 075422 (2016).
[86] G. Rupper, S. Rudin, and M. S. Shur, Phys. Rev. Appl. **9**, 064007 (2018).
[87] E. Mönch, S. O. Potashin, K. Lindner, I. Yahniuk, L. E. Golub, V. Y. Kachorovskii, V. V. Bel'kov, R. Huber, K. Watanabe, T. Taniguchi, J. Eroms, D. Weiss, and S. D. Ganichev, Phys. Rev. B **105**, 045404 (2022).
[88] E. Mønch, S. O. Potashin, K. Lindner, I. Yahniuk, L. E. Golub, V. Y. Kachorovskii, V. V. Bel'kov, R. Huber, K. Watanabe, T. Taniguchi, J. Eroms, D. Weiss, and S. D. Ganichev, arXiv:2208.08299.
[89] C. Q. Cook and A. Lucas, Phys. Rev. B **99**, 235148 (2019).
[90] G. Varnavides, A. S. Jermyn, P. Anikeeva, C. Felser, and P. Narang, Nat. Commun. **11**, 4710 (2020).
[91] P. Rao and B. Bradlyn, Phys. Rev. X **10**, 021005 (2020).
[92] I. n. Robredo, P. Rao, F. de Juan, A. Bergara, J. L. Mañes, A. Cortijo, M. G. Vergniory, and B. Bradlyn, Phys. Rev. Res. **3**, L032068 (2021).
[93] P. Rao and B. Bradlyn, arXiv:2112.04545.
[94] J. M. Link and I. F. Herbut, Phys. Rev. B **101**, 125128 (2020).
[95] G. Varnavides, A. S. Jermyn, P. Anikeeva, C. Felser, and P. Narang, arXiv:2002.08976.
[96] R. Toshio, K. Takasan, and N. Kawakami, Phys. Rev. Res. **2**, 032021(R) (2020).
[97] H. Funaki and G. Tatara, Phys. Rev. Res. **3**, 023160 (2021).
[98] H. Funaki, R. Toshio, and G. Tatara, Phys. Rev. Res. **3**, 033075 (2021).
[99] G. Tatara, Phys. Rev. B **104**, 184414 (2021).
[100] O. Tavakol and Y. B. Kim, Phys. Rev. Res. **3**, 013290 (2021).
[101] E. H. Hasdeo, J. Ekström, E. G. Idrisov, and T. L. Schmidt, Phys. Rev. B **103**, 125106 (2021).
[102] R. Sano, R. Toshio, and N. Kawakami, Phys. Rev. B **104**, L241106 (2021).
[103] Y. Wang, G. Varnavides, R. Sundararaman, P. Anikeeva, J. Gooth, C. Felser, and P. Narang, Phys. Rev. Mater. **6**, 083802 (2022).
[104] G. Varnavides, A. S. Jermyn, P. Anikeeva, and P. Narang, arXiv:2204.06004.
[105] G. Varnavides, Y. Wang, P. J. W. Moll, P. Anikeeva, and P. Narang, Phys. Rev. Mater. **6**, 045002 (2022).
[106] X. Huang and A. Lucas, J. High Energy Phys. 03 (2022) 082.
[107] A. J. Friedman, C. Q. Cook, and A. Lucas, arXiv:2202.08269.
[108] R. Sano, D. Oue, and M. Matsuo, arXiv:2204.02409.
[109] M. Z. Hasan and C. L. Kane, Rev. Mod. Phys. **82**, 3045 (2010).
[110] T. Stauber, J. Phys.: Condens. Matter **26**, 123201 (2014).
[111] B. Yan and C. Felser, Annu. Rev. Condens. Matter Phys. **8**, 337 (2017).
[112] F. M. D. Pellegrino, M. I. Katsnelson, and M. Polini, Phys. Rev. B **92**, 201407(R) (2015).
[113] J. C. W. Song and M. S. Rudner, Proc. Natl. Acad. Sci. USA **113**, 4658 (2016).
[114] J. Hofmann and S. Das Sarma, Phys. Rev. B **93**, 241402(R) (2016).
[115] A. Kumar, A. Nemilentsau, K. H. Fung, G. Hanson, N. X. Fang, and T. Low, Phys. Rev. B **93**, 041413(R) (2016).
[116] X. Lu, D. K. Mukherjee, and M. O. Goerbig, Phys. Rev. B **104**, 155103 (2021).
[117] Although here we have neglected the high-harmonic modulations [122,124,126] for simplicity, we will consider them in the following. As also noted in Ref. [84], the field amplitude $\tilde{\boldsymbol{E}}_0$ should be smaller than the amplitude of the incident field due to the screening by the gates in reality. Moreover, in general, the grating parameter $\hat{h}$ strongly depends on frequencies [85,122]. Nevertheless, we believe that our simplified model captures the key physics of the problem and is sufficient for clarifying the interplay between plasmonic nanostructures and quantum geometrical effects.
[118] M. Shur, *GaAs Devices and Circuits* (Plenum, New York, 1987).
[119] L. D. Landau and E. M. Lifshitz, *Course of Theoretical Physics: Fluid Mechanics*, 2nd ed. (Pergamon, New York, 1987).
[120] See Supplemental Material at http://link.aps.org/supplemental/10.1103/PhysRevB.106.L201301 for details.
[121] Our definition of $\boldsymbol{M}$ is different from the one in Ref. [102] by a constant factor $m\hbar/e$.
[122] V. V. Popov, D. V. Fateev, E. L. Ivchenko, and S. D. Ganichev, Phys. Rev. B **91**, 235436 (2015).
[123] T. W. W. Maß, V. H. Nguyen, U. Schnakenberg, and T. Taubner, Opt. Express **27**, 10524 (2019).
[124] V. V. Popov, O. V. Polischuk, T. V. Teperik, X. G. Peralta, S. J. Allen, N. J. M. Horing, and M. C. Wanke, J. Appl. Phys. **94**, 3556 (2003).
[125] D. V. Fateev, V. V. Popov, and M. S. Shur, Semiconductors **44**, 1406 (2010).
[126] E. L. Ivchenko and M. I. Petrov, Phys. Solid State **56**, 1833 (2014).
[127] A. V. Muravjov, D. B. Veksler, V. V. Popov, O. V. Polischuk, N. Pala, X. Hu, R. Gaska, H. Saxena, R. E. Peale, and M. S. Shur, Appl. Phys. Lett. **96**, 042105 (2010).
[128] N. Guo, W.-D. Hu, X.-S. Chen, L. Wang, and W. Lu, Opt. Express **21**, 1606 (2013).
[129] K. Li, J. M. Fitzgerald, X. Xiao, J. D. Caldwell, C. Zhang, S. A. Maier, X. Li, and V. Giannini, ACS Omega **2**, 3640 (2017).
[130] J. T. Hugall, A. Singh, and N. F. van Hulst, ACS Photon. **5**, 43 (2018).
[131] X. Xiao, X. Li, J. D. Caldwell, S. A. Maier, and V. Giannini, Appl. Mater. Today **12**, 283 (2018).
[132] I. Epstein, D. Alcaraz, Z. Huang, V.-V. Pusapati, J.-P. Hugonin, A. Kumar, X. M. Deputy, T. Khodkov, T. G. Rappoport, J.-Y. Hong, N. M. R. Peres, J. Kong, D. R. Smith, and F. H. L. Koppens, Science **368**, 1219 (2020).
[133] Z. Ullah, G. Witjaksono, I. Nawi, N. Tansu, M. Irfan Khattak, and M. Junaid, Sensors **20**, 1401 (2020).
[134] In the case of y-polarized incident light, Hall currents induced by the oscillating magnetic field, which causes spatially dispersive terms such as $\boldsymbol{j}_{\rm DC}^{\rm Lorentz}$, slightly break this relation. Furthermore, since we use the fact that the particle density n

is spatially uniform in equilibrium to take it outside of $\langle \cdots \rangle_{t,r}$, this relation will break in the case in which strong static built-in fields are applied on the 2D electron systems by a periodic doping gate as investigated in Refs. [81,84].

[135] Y. Onishi, H. Watanabe, T. Morimoto, and N. Nagaosa, arXiv:2204.12727.

[136] L. kun Shi, O. Matsyshyn, J. C. W. Song, and I. S. Villadiego, arXiv:2207.03496.

[137] Q. Ma, S.-Y. Xu, H. Shen, D. MacNeill, V. Fatemi, T.-R. Chang, A. M. Mier Valdivia, S. Wu, Z. Du, C.-H. Hsu, S. Fang, Q. D. Gibson, K. Watanabe, T. Taniguchi, R. J. Cava, E. Kaxiras, H.-Z. Lu, H. Lin, L. Fu, N. Gedik, et al., Nature (London) **565**, 337 (2019).

[138] G. Auton, J. Zhang, R. K. Kumar, H. Wang, X. Zhang, Q. Wang, E. Hill, and A. Song, Nat. Commun. **7**, 11670 (2016).

[139] C.-P. Zhang, J. Xiao, B. T. Zhou, J.-X. Hu, Y.-M. Xie, B. Yan, and K. T. Law, Phys. Rev. B **106**, L041111 (2022).

[140] Here we have neglected the term proportional to geometrical scalar Y for simplicity, since it is a higher-order spatially dispersive term, which is proportional to q^4, and thus much smaller than other terms for typical values of q.

[141] S.-Y. Xu, Q. Ma, H. Shen, V. Fatemi, S. Wu, T.-R. Chang, G. Chang, A. M. M. Valdivia, C.-K. Chan, Q. D. Gibson, J. Zhou, Z. Liu, K. Watanabe, T. Taniguchi, H. Lin, R. J. Cava, L. Fu, N. Gedik, and P. Jarillo-Herrero, Nat. Phys. **14**, 900 (2018).

[142] D. A. Bandurin, I. Torre, R. K. Kumar, M. Ben Shalom, A. Tomadin, A. Principi, G. H. Auton, E. Khestanova, K. S. Novoselov, I. V. Grigorieva, L. A. Ponomarenko, A. K. Geim, and M. Polini, Science **351**, 1055 (2016).

[143] J. Crossno, J. K. Shi, K. Wang, X. Liu, A. Harzheim, A. Lucas, S. Sachdev, P. Kim, T. Taniguchi, K. Watanabe, T. A. Ohki, and K. C. Fong, Science **351**, 1058 (2016).

[144] R. K. Kumar, D. Bandurin, F. Pellegrino, Y. Cao, A. Principi, H. Guo, G. Auton, M. B. Shalom, L. A. Ponomarenko, G. Falkovich *et al.*, Nat. Phys. **13**, 1182 (2017).

[145] D. A. Bandurin, A. V. Shytov, L. S. Levitov, R. K. Kumar, A. I. Berdyugin, M. Ben Shalom, I. V. Grigorieva, A. K. Geim, and G. Falkovich, Nat. Commun. **9**, 4533 (2018).

[146] J. A. Sulpizio, L. Ella, A. Rozen, J. Birkbeck, D. J. Perello, D. Dutta, M. Ben-Shalom, T. Taniguchi, K. Watanabe, T. Holder, R. Queiroz, A. Principi, A. Stern, T. Scaffidi, A. K. Geim, and S. Ilani, Nature (London) **576**, 75 (2019).

[147] A. I. Berdyugin, S. G. Xu, F. M. D. Pellegrino, R. Krishna Kumar, A. Principi, I. Torre, M. Ben Shalom, T. Taniguchi, K. Watanabe, I. V. Grigorieva, M. Polini, A. K. Geim, and D. A. Bandurin, Science **364**, 162 (2019).

[148] L. W. Molenkamp and M. J. M. de Jong, Phys. Rev. B **49**, 5038 (1994).

[149] M. J. M. de Jong and L. W. Molenkamp, Phys. Rev. B **51**, 13389 (1995).

[150] B. A. Braem, F. M. D. Pellegrino, A. Principi, M. Röösli, C. Gold, S. Hennel, J. V. Koski, M. Berl, W. Dietsche, W. Wegscheider, M. Polini, T. Ihn, and K. Ensslin, Phys. Rev. B **98**, 241304(R) (2018).

[151] G. M. Gusev, A. D. Levin, E. V. Levinson, and A. K. Bakarov, AIP Adv. **8**, 025318 (2018).

[152] G. M. Gusev, A. D. Levin, E. V. Levinson, and A. K. Bakarov, Phys. Rev. B **98**, 161303(R) (2018).

[153] A. D. Levin, G. M. Gusev, E. V. Levinson, Z. D. Kvon, and A. K. Bakarov, Phys. Rev. B **97**, 245308 (2018).

[154] P. J. W. Moll, P. Kushwaha, N. Nandi, B. Schmidt, and A. P. Mackenzie, Science **351**, 1061 (2016).

[155] J. Gooth, F. Menges, C. Shekhar, V. S. N. Kumar, Y. Sun, U. Drechsler, R. Zierold, C. Felser, and B. Gotsmann, Nat. Commun. **9**, 4093 (2018).

[156] U. Vool, A. Hamo, G. Varnavides, Y. Wang, T. X. Zhou, N. Kumar, Y. Dovzhenko, Z. Qiu, C. A. C. Garcia, A. T. Pierce, J. Gooth, P. Anikeeva, C. Felser, P. Narang, and A. Yacoby, Nat. Phys. **17**, 1216 (2021).

[157] Y.-G. Choi, M.-H. Doan, G.-M. Choi, and M. N. Chernodub, arXiv:2201.08331.

[158] A. Aharon-Steinberg, T. Vlkl, A. Kaplan, A. K. Pariari, I. Roy, T. Holder, Y. Wolf, A. Y. Meltzer, Y. Myasoedov, M. E. Huber, B. Yan, G. Falkovich, L. S. Levitov, M. Hücker, and E. Zeldov, Nature **607**, 74 (2022).

[159] H. Wang and X. Qian, npj Comput. Mater. **5**, 119 (2019).

[160] K. Kang, T. Li, E. Sohn, J. Shan, and K. F. Mak, Nat. Mater. **18**, 324 (2019).

[161] S.-C. Ho, C.-H. Chang, Y.-C. Hsieh, S.-T. Lo, B. Huang, T.-H.-Y. Vu, C. Ortix, and T.-M. Chen, Nat. Electron. **4**, 116 (2021).

[162] Z. He and H. Weng, npj Quantum Mater. **6**, 101 (2021).

[163] J. E. Moore and J. Orenstein, Phys. Rev. Lett. **105**, 026805 (2010).

[164] S. D. Ganichev, E. L. Ivchenko, S. N. Danilov, J. Eroms, W. Wegscheider, D. Weiss, and W. Prettl, Phys. Rev. Lett. **86**, 4358 (2001).

[165] H. Diehl, V. A. Shalygin, V. V. Bel'kov, C. Hoffmann, S. N. Danilov, T. Herrle, S. A. Tarasenko, D. Schuh, C. Gerl, W. Wegscheider, W. Prettl, and S. D. Ganichev, New J. Phys. **9**, 349 (2007).

[166] P. Olbrich, S. A. Tarasenko, C. Reitmaier, J. Karch, D. Plohmann, Z. D. Kvon, and S. D. Ganichev, Phys. Rev. B **79**, 121302(R) (2009).

[167] M. Zarenia, I. Yudhistira, S. Adam, and G. Vignale, Phys. Rev. B **101**, 045421 (2020).

[168] Y. Cao, D. Chowdhury, D. Rodan-Legrain, O. Rubies-Bigorda, K. Watanabe, T. Taniguchi, T. Senthil, and P. Jarillo-Herrero, Phys. Rev. Lett. **124**, 076801 (2020).

[169] J. González and T. Stauber, Phys. Rev. Lett. **124**, 186801 (2020).

[170] P. Cha, A. A. Patel, and E.-A. Kim, Phys. Rev. Lett. **127**, 266601 (2021).

[171] S. Das Sarma and F. Wu, Phys. Rev. Res. **4**, 033061 (2022).

[172] Z. Qian and G. Vignale, Phys. Rev. B **71**, 075112 (2005).

[173] P. S. Alekseev, Phys. Rev. Lett. **117**, 166601 (2016).

[174] R. A. Davison, K. Schalm, and J. Zaanen, Phys. Rev. B **89**, 245116 (2014).

[175] P. K. Kovtun, D. T. Son, and A. O. Starinets, Phys. Rev. Lett. **94**, 111601 (2005).

[176] M. Freitag, T. Low, W. Zhu, H. Yan, F. Xia, and P. Avouris, Nat. Commun. **4**, 1951 (2013).

[177] J. Guo, R. Xiang, T. Cheng, S. Maruyama, and Y. Li, ACS Nanosci. Au **2**, 3 (2022).

[178] T.-T. Kim, S. S. Oh, H.-D. Kim, H. S. Park, O. Hess, B. Min, and S. Zhang, Sci. Adv. **3**, e1701377 (2017).

[179] H. Shokri Kojori, J.-H. Yun, Y. Paik, J. Kim, W. A. Anderson, and S. J. Kim, Nano Lett. **16**, 250 (2016).

[180] M. Kolodrubetz, V. Gritsev, and A. Polkovnikov, Phys. Rev. B **88**, 064304 (2013).